Physicalist Computational Structures for Motion Perception in Mammal Visual Cortex

Silvio P. Sabatini, Paolo Cavalleri, Fabio Solari, Giacomo M. Bisio

Department of Biophysical and Electronic Engineering
University of Genoa, I-16145 Genova, ITALY - *silvio@dibe.unige.it*

1 Introduction

Information about relative motion between an observer and the environment are extracted from the optic flow at different stages of cortical visual processing, going from the primary visual cortex (V1), through the middle temporal area (MT), to the medial superior temporal area (MST). Ascension towards extrastriate areas is characterized by a systematic increase in receptive field size and complexity, corresponding to a progressive increment of their representation properties. Specifically, the sensitivity to large-field complex motion stimuli, such as rotation and expansion/contraction [Duffy and Wurtz, 1991] [Tanaka and Saito, 1989] [Graziano *et al.*, 1994] [Orban, 1992], in the dorsal portion of the medial superior temporal area (MSTd) supports the view that MST is suited for the analysis of wide-field egomotion induced by head and body movements.
Although there is little doubt that the brain uses some kind of optic flow information when looking at moving stimuli, it is not clear how the brain represents and analyzes optic flow fields. In a computational perspective it has been shown that locally a smooth optic flow field can be approximated by its first-order spatial derivatives or elementary flow components, identified by vector operators div, curl, and def, to be related to expansion, rotation, and shear deformation, respectively [Koenderink, 1986]. Behavioural properties of MST cells, as postulated by such vector calculus, would imply a degree of functional specificity which might be higher than what can be determined genetically or learned by experience.
However, it is not necessary for any physiological system to be able to compute pure vectorial quantities, but it is sufficient to approximate them, at a subsymbolic level, through spatiotemporal operators, taking advantage of retinocortical mapping and of a proper representation of the optic flow. To this goal, in this paper we propose a physicalist model of extrastriate cortical motion processing where optic flow invariants are mapped as spatiotemporal patterns of activation on a log-polar MT representation, and MST processing is modeled by spatiotemporal filtering operators. Such spatiotemporal filters perform a local analysis of the optic flow, but as a whole they make available information about the global structure of the optic flow and thus about the motion parameters, that define heading. The characteristic features of our MST-like units, that resemble those

observed in real cells, result as emerging properties of the geometrical organization of our model.

2 Computational structures for heading estimation

2.1 The problem

When an observer moves through the environment the projection of the three-dimensional (3-D) world on his retina changes continuously. As Gibson [Gibson, 1950] observed, the changing retinal image gives raise to the optic flow, as a two-dimensional (2-D) vectorial field where each vector encodes the direction and speed of displacement for each point in the visual field (x, y). In the 3-D world the motion of an observer is specified by the translational velocity $\mathbf{T} = (T_X, T_Y, T_Z)$ and the rotational velocity $\mathbf{\Omega} = (\Omega_X, \Omega_Y, \Omega_Z)$. The optic flow experienced during egomotion can be expressed in each point of the retinal plane as [Heeger and Jepson, 1990]:

$$\mathbf{v}(x, y) = p(x, y)\mathbf{A}(x, y)\mathbf{T} + \mathbf{B}(x, y)\mathbf{\Omega} \tag{1}$$

where $p(x, y) = 1/Z$ is the inverse depth of the object projecting in (x, y),

$$\begin{aligned} \mathbf{A}(x, y) &= \begin{pmatrix} -f & 0 & x \\ 0 & -f & y \end{pmatrix} \\ \mathbf{B}(x, y) &= \begin{pmatrix} (xy)/f & -(f + x^2/f) & y \\ f + y^2/f & -(xy)/f & -x \end{pmatrix} \end{aligned}$$

and f is the focal length of the optical system.
If no eye rotation occurs and the observer moves along a straight line in a static scene (i.e., $\mathbf{\Omega} = 0$), the optic flow presents a radial pattern flowing out from a point commonly named *focus of expansion*. This singularity point corresponds to the projection of the heading direction on the image plane, at its spatial location $(f\frac{T_X}{T_Z}, f\frac{T_Y}{T_Z})$ where $\mathbf{v} = 0$.

2.2 Centric-minded operators

Retino-cortical mapping A log-polar transformation provides an accepted model of the mapping from the retina to the visual cortex in primates at both local and global scales [Schwartz, 1977]. Considering the radiality of the optic flow patterns during egomotion, the presence of such a retino-cortical mapping greatly simplifies their cortical representations and, in general, the geometry of the problem. In this way, indeed, fovea-centered expansive and rotatory flow fields are mapped into space-variant translational velocity patterns according to a criterium of uniform allocation of resources on the cortical surface. In other words such polar mapping separates locally the angular and radial components of image velocities and allows, through its log-scaling property, an almost invariant representation of the global flow patterns. Formally, the topological transformation from the retinal plane (x, y) to the cortical plane (ξ, θ), can be formulated as follows [Tistarelli and Sandini, 1993]:

$$\begin{cases} \xi = \log(r + a) = \log(\sqrt{x^2 + y^2} + a) \\ \theta = \theta = \arctan(y/x) \end{cases}$$

where a is a small real constant to make the mapping regular at the origin. Consequently the transformation of velocity from the cartesian to the log-polar plane is:

$$\begin{bmatrix} \dot{\xi} \\ \dot{\theta} \end{bmatrix} = \begin{bmatrix} \mathrm{e}^{-\xi}\cos\theta & \mathrm{e}^{-\xi}\sin\theta \\ -\frac{\sin\theta}{\mathrm{e}^{\xi}-a} & \frac{\cos\theta}{\mathrm{e}^{\xi}-a} \end{bmatrix} \begin{bmatrix} \dot{x} \\ \dot{y} \end{bmatrix} \tag{2}$$

and it is possible to rewrite the optic flow relation (1) as:

$$\begin{cases} \dot{\xi} = -fP(\xi)\left[\frac{T_X}{Z} + R(\xi)\Omega_Y\right]\cos\theta - fP(\xi)\left[\frac{T_Y}{Z} - R(\xi)\Omega_X\right]\sin\theta + \frac{P(\xi)}{Q(\xi)}\frac{T_Z}{Z} \\ \dot{\theta} = fQ(\xi)\left(\frac{T_X}{Z} + \Omega_Y\right)\sin\theta - fQ(\xi)\left(\frac{T_Y}{Z} - \Omega_X\right)\cos\theta - \Omega_Z \end{cases} \tag{3}$$

where $P(\xi) = \mathrm{e}^{-\xi}$, $Q(\xi) = (\mathrm{e}^{\xi} - a)^{-1}$ and $R(\xi) = 1 + (\mathrm{e}^{\xi} - a)^2/f^2$.
Eqs. (3) in log-polar coordinates provide a very clear representation of the relationship existing between the act of motion of the observer and the structure of the optic flow field. Assuming, for sake of argument, that Z, the depth of object is independent of ξ and θ, a simple translational movement in the direction of gaze ($T_Z \neq 0$) will generate a uniform radial field, $\dot{\xi} = \text{const}$. Translation movement with T_X OR $T_Y \neq 0$ will generate fields with radial component, $\dot{\xi}$, depending on θ and tangential component, $\dot{\theta}$, depending also on θ.
Direction of heading can be recovered by the degree of deviation of the optic flow from a radial flow centered on the fovea. Such deviations result in radial asymmetries of the velocity vector field in both direction and magnitude. In fact, if the direction of gaze and the direction of movement are coincident, resulting in a null gaze-movement angle, then the velocity flow field is symmetric with respect to both the directions and the magnitudes of image element trajectories. As gaze-movement angle increases, the asymmetry in the distribution of image velocities also increases and such asymmetries can be used to determine heading. In particular, several authors (e.g. [Dyre and Andersen, 1997]) suggested that the observer could use the asymmetries in the retinal flow pattern to guide a sequence of fixations until the distribution of image velocity is symmetric, resulting in the coincidence of the directions of movement and gaze. This approach has received relatively little attention in the literature about heading, though it may have a number of interesting functional implications for purposive active vision in relation to the problem of understanding how and by which cortical mechanisms the visual system contributes to proprioception.

Weight vector templates To take advantage of the geometrical properties of the log-polar mapping, we adopt a gaze-centered approach, in which the optic flow is analyzed in terms of how it is related to the fixation point. Accordingly, asymmetries in the field distribution are analyzed in the neighbourhood of each location $\mathbf{r} = (r, \theta)$ of the retinal plane through two independent sets of operators sensitive to radial and rotational patterns around the fovea, respectively:

$$\begin{aligned} \mathrm{e}_{\mathrm{EXP}}(\mathbf{r}) &= \int_{\mathrm{S}(\mathbf{r})} \mathbf{h}_{\mathrm{EXP}}(\mathbf{r}') \cdot \mathbf{v}(\mathbf{r}')\mathrm{d}\mathbf{r}' \\ \mathrm{e}_{\mathrm{ROT}}(\mathbf{r}) &= \int_{\mathrm{S}(\mathbf{r})} \mathbf{h}_{\mathrm{ROT}}(\mathbf{r}') \cdot \mathbf{v}(\mathbf{r}')\mathrm{d}\mathbf{r}' \end{aligned} \tag{4}$$

These two operators represent abstract cortical cells that integrate, over a limited spatial domain $S(\mathbf{r})$ (i.e. their receptive fields), the dot product between the optic flow field and

a set of weight vector fields of unitary expansion and rotation rate, defined as:

$$\mathbf{h}_{\mathrm{EXP}}(\mathbf{r}) = \frac{1}{2}\mathbf{r} \quad \text{and} \quad \mathbf{h}_{\mathrm{ROT}}(\mathbf{r}) = \frac{1}{2}\mathbf{n} \wedge \mathbf{r} \tag{5}$$

where $\boldsymbol{n}$ is the unit vector perpendicular to the image plane. These operators act as matched filters detecting the presence of a particular directional pattern within the perceived optic flow and producing their maximal output when the local flow vectors are parallel to the weight vector fields. Notwithstanding their limited extension in space, such centric-minded operators, extract, as a whole, global information from the input flow field, being sensitive to different local instances of the same global property of the vector field with respect to the fixation point (see Section 3).

2.3 Physicalist computation, or How to approximate vector calculus in the parametric space through integral operations in space-time

Wave-like representation Following a *Gestalt* approach, we assume that the cortical code of the optic flow field should represent morphologically the triggering perceptual event (i.e., the spatiotemporal structure of the optic array, cf. [Gibson, 1950]). This problem can be embodied by the *isomorphism principle* [Kohler, 1947] asserting that perception takes place when systems reactions occur isomorphically to the impinging pattern of activation, i.e., the reacting brain process have the same structure as the perceptual event it gave rise to. Accordingly, we formulate the hypothesis that, at MT level, a "motion event" in the visual space is isomorphycally associated to a "motion event" on the cortical surface. More specifically, the activation of a pool of MT cells by a coherent motion pattern yields, on a macroscopic scale, a spatiotemporal pattern in the form of a wave representing with its flow the vectorial information. Formally, to each vector $\mathbf{v}(\mathbf{z}')$ of the optic flow we associate a localized traveling wave centered around the cortical location $\mathbf{z}' = (\xi', \theta')$:

$$g(\mathbf{z} - \mathbf{z}', t) = \frac{1}{2\pi\sigma^2} \exp\left(-\frac{|\mathbf{z} - \mathbf{z}'|^2}{2\sigma^2}\right) \cos\left[\mathbf{k}(\mathbf{z}') \cdot ((\mathbf{z} - \mathbf{z}') - \mathbf{v}(\mathbf{z}')t)\right] \tag{6}$$

where $\mathbf{k}$ is a two-dimensional (2D) spatial frequency vector oriented as $\mathbf{v}$ with a modulus $|\mathbf{k}|$ independent of $\mathbf{z}'$. Each wave extends over a spatial region determined by σ and overlaps with waves at nearby locations. The interference pattern obtained, at each location, by integrating partially overlapping waves across a spatial domain S, is defined as the *cortical flow*:

$$f(\mathbf{z}, t) = \int_S g(\mathbf{z} - \mathbf{z}', t)\mathrm{d}\mathbf{z}' \tag{7}$$

and can be interpreted as a spatiotemporal cortical correlate of the input vector field $\mathbf{v}$ [1]. As shown in Fig. 1, ordered spatial configurations of the velocity field $\mathbf{v}$ correspond to ordered spatiotemporal configurations of the cortical flow $f(\mathbf{z}, t)$, thus indicating that such representation preserves qualitative properties of the optic flow.

[1] The cortical flow hypothesis starts from a speculation, partially supported by experimental evidence that when a subject is stimulated by motion stimuli, ordered patterns of dynamic activations arise within retinotopically organized visual areas. These activations should be intended as a macroscopic (i.e, averaged) activity that can be compared to spatiotemporal flow of excitation revealed by current source density analysis, local field potentials, optical imaging, or, at higher scales of observations by fMRI.

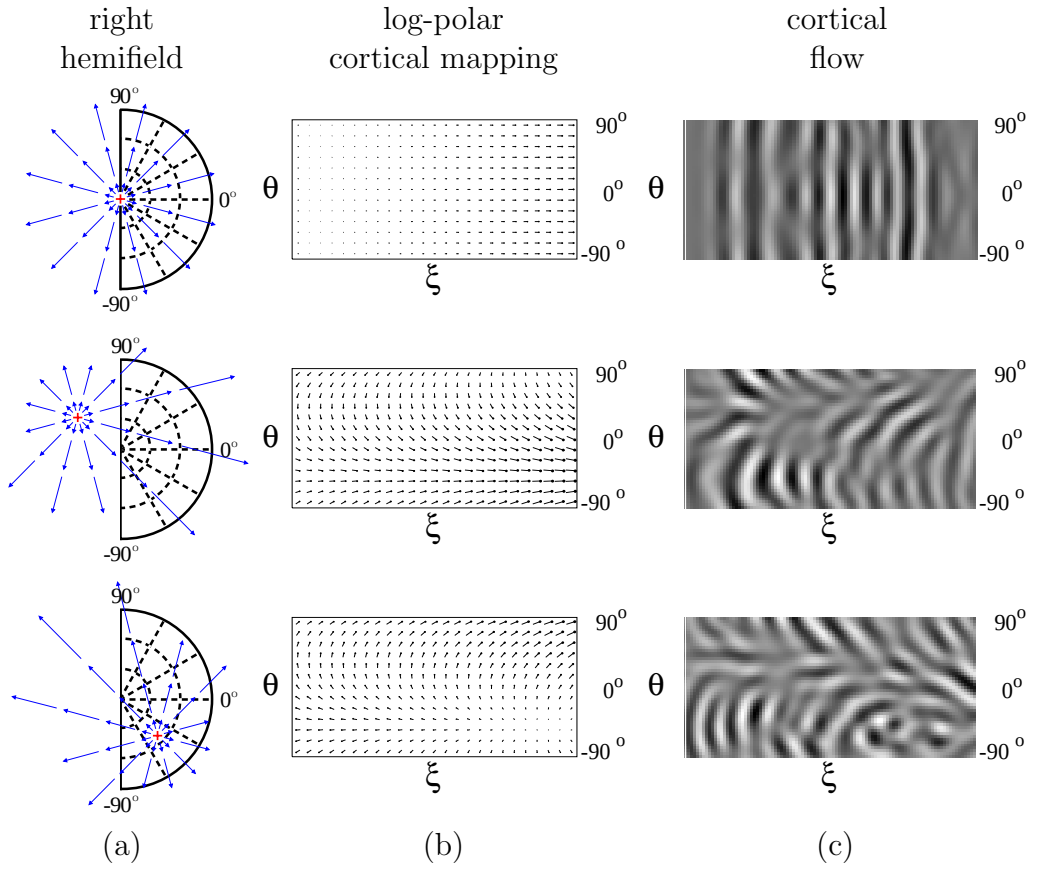

Figure 1: (a) Optic flow stimuli corresponding to expansions with differently shifted center of motion. (b) Corresponding log-polar mapping. (c) "Snapshots" of the related cortical flow representations in area MT (see text).

Spatiotemporal filtering On the basis of the geometry of the log-polar mapping and of the spatiotemporal representation of the optic flow, introduced in the previous Section, it is possible to derive a scheme for approximating the vector templates in terms of spatiotemporal filtering operators characterized by directionally-tuned kernels $h(\mathbf{z}, t)$ to detect translational motion of the cortical flow. Specifically, we consider rightward and leftward motion filters for expansion and contraction, and downward and upward motion filters for clockwise and counterclockwise rotations, respectively (see Fig. 2b). The approach can be straightforwardly generalized to combinations of rotation and expansion/contraction, i.e., to spiral motions [Graziano *et al.*, 1994], by considering filters oriented along oblique directions. The level of activity of an MST neuron is given by:

$$e_{mst}(\mathbf{z}, t) = \int f(\mathbf{z} - \mathbf{z}', t - t')h(\mathbf{z}', t')\mathrm{d}\mathbf{z}'\mathrm{d}t', \tag{8}$$

with matching filters $h(\mathbf{z}, t)$ specified as localized waves damped in time:

$$h(\mathbf{z}, t) = \frac{1}{2\pi\sigma_h^2} \exp\left(-\frac{|\mathbf{z}|^2}{2\sigma_h^2} - \frac{t}{\tau}\right) \cos[\mathbf{k}_h \cdot (\mathbf{z} - \mathbf{v}_h t)] \tag{9}$$

where τ is a decay constant, $\mathbf{k}_h$ is the 2D spatial frequency vector, $\mathbf{v}_h$ is related to the cell's speed sensitivity, and σ_h specifies the spatial extension of the integration area over MT

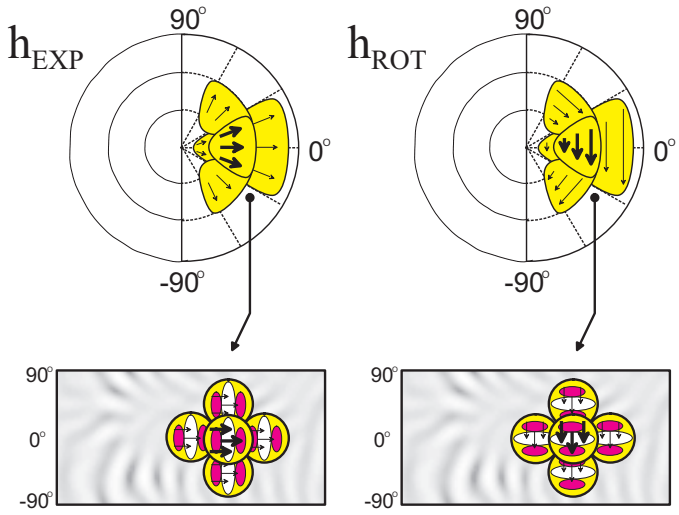

Figure 2: An illustration of the template matching between an expansion-selective cell and an optic flow field with a shifted center of motion. The shaded region indicates the cell's receptive field and the thick vectors indicate its preference for expansion. Vector operations performed by the templates for expansion-selective and for rotation-selective cells are reduced to filtering operations to detect translational motion of the cortical flow.

representation, and it is ultimately related to the size of MST receptive fields. For dilation filters $\mathbf{k}_h = (k_{h\xi}, 0)$, $\mathbf{v}_h = (v_{h\xi}, 0)$ with $v_{h\xi} > 0$ for expansion and $v_{h\xi} < 0$ for contraction. For rotation filters $\mathbf{k}_h = (0, k_{h\theta})$, $\mathbf{v}_h = (0, v_{h\theta})$ with $v_{h\theta} > 0$ for counterclockwise rotation and $v_{h\theta} < 0$ for clockwise rotation.

3 Results

Since the global structure of the optic flow is analysed by means of local operators, it is necessary to observe the outputs of a pool of cells distributed all over the visual field to estimate egomotion parameters. The distribution of activity, characterized by a marked anisotropy when the focus of expansion is peripheral, turns to be isotropic (i.e., independent of the angular coordinate of the receptive field) as the focus moves toward the center of the visual field. As shown in Fig. 3, the activity distribution of expansion cells reaches a peak, at θ_1, in the region where the optic flow is maximally radial, i.e., in the region opposite to the position of the focus of expansion (θ_p) respect to the fovea: $(\theta_p - \theta_1) = \pi$. For the cells selective to rotational flow the distribution of activity still peaks in a particular location, θ_2, when the focus is in the periphery, but the angle between the focus and the activity peak is $(\theta_p - \theta_2) = \pi/2$, instead of π. By analyzing such distribution of activities it is possible to make a prediction about heading: the angular position of their peaks locates the visual direction of heading:

$$\arctan \frac{T_Y}{T_X} = \theta_1 + \pi \quad ; \quad \arctan \frac{T_Y}{T_X} = \theta_2 + \frac{\pi}{2}$$

and their degree of isotropy gives information on the value of the angle between the direction of heading and the direction of gaze.
To quantitatively assess the performance of the model we show how the activity distribution of a population of model cells can be used to gain information about global motion

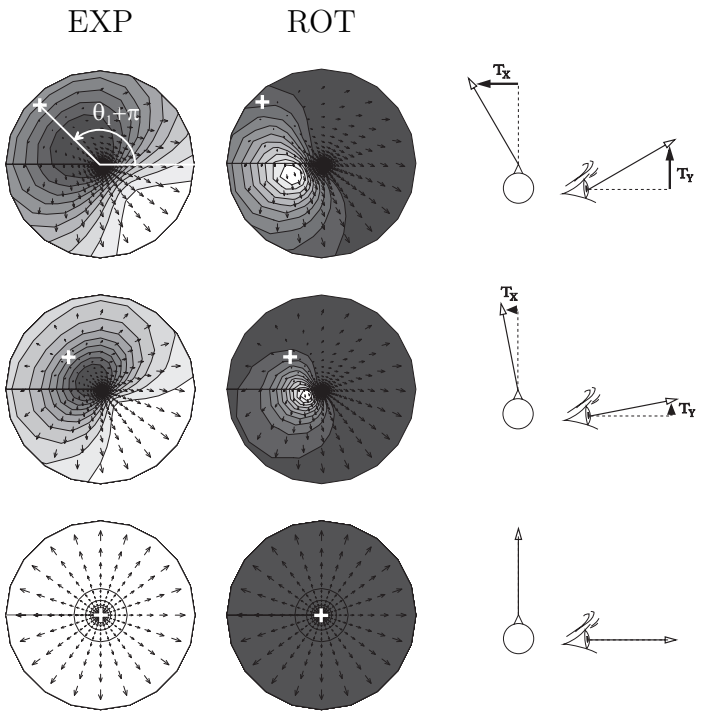

Figure 3: Distributions of the filter responses. The grey level indicates the activity of each unit in the corresponding location. The filters' outputs can be directly used in a control loop scheme to guide the direction of gaze (dashed lines) towards the direction of heading (solid lines) (see text). The white crosses evidence the position of the focus of expansion.

parameters. To this purpose, it is convenient to take advantage of the log-polar mapping and to define the gaze-centered weight vector fields (Eqs. (5)) in the cortical plane:

$$\mathbf{h}_{\mathrm{EXP}}(\xi,\theta) = \left[0.5(1-a\mathrm{e}^{-\xi}),0\right] \simeq (0.5,0)\,; \quad \mathbf{h}_{\mathrm{ROT}}(\xi,\theta) = (0,0.5)$$

evidencing that their specific tuning for radial and angular (i.e., tangential) components of the optic flow result in the cortical plane in uniform fields directed along the ξ and θ axes, respectively. In the cortical plane Eq. 4 becomes:

$$\mathrm{e}_{\mathrm{EXP}}(\xi,\theta) = \int_{\mathrm{S}} \mathbf{h}_{\mathrm{EXP}}(\xi',\theta')\cdot\mathbf{v}(\xi',\theta')\mathrm{d}\xi'\mathrm{d}\theta' \tag{10}$$

$$\mathrm{e}_{\mathrm{ROT}}(\xi,\theta) = \int_{\mathrm{S}} \mathbf{h}_{\mathrm{ROT}}(\xi',\theta')\cdot\mathbf{v}(\xi',\theta')\mathrm{d}\xi'\mathrm{d}\theta' \tag{11}$$

where $\mathbf{v} \stackrel{def}{=} (\dot{\xi},\dot{\theta})$, see Eq. 3. In the case of passive navigation ($\mathbf{\Omega}=0$), one has:

$$\mathrm{e}_{\mathrm{EXP}}\left(\xi,\theta;\frac{T_X}{T_Z},\frac{T_Y}{T_Z}\right) = \frac{T_Z}{\tilde{Z}}\left[Q_1(\xi)\left(-\frac{T_X}{T_Z}\cos\theta-\frac{T_Y}{T_Z}\sin\theta\right)+Q_2(\xi)\right] \tag{12}$$

$$\mathrm{e}_{\mathrm{ROT}}\left(\xi,\theta;\frac{T_X}{T_Z},\frac{T_Y}{T_Z}\right) = \frac{T_Z}{\tilde{Z}}\left[P_1(\xi)\left(\frac{T_X}{T_Z}\sin\theta-\frac{T_Y}{T_Z}\cos\theta\right)\right] \tag{13}$$

where $P_1(\xi)$, $Q_1(\xi)$ and $Q_2(\xi)$ are quantities depending on the position and spatial extension of the receptive fields, and $\tilde{Z}$ is a weighted average of the depth of objects in the domain specified by S.

From Eqs. (12) and (13) one can directly analyze the tuning properties of expansion and rotation selective cells to heading direction $(\frac{T_X}{T_Z}, \frac{T_Y}{T_Z})$. Each cell response, as a function of $(\frac{T_X}{T_Z}, \frac{T_Y}{T_Z})$, is described by a linear expression parametrized by coefficients that depend on the cell's cortical location (ξ, θ), where the dependence on θ is the most relevant one.

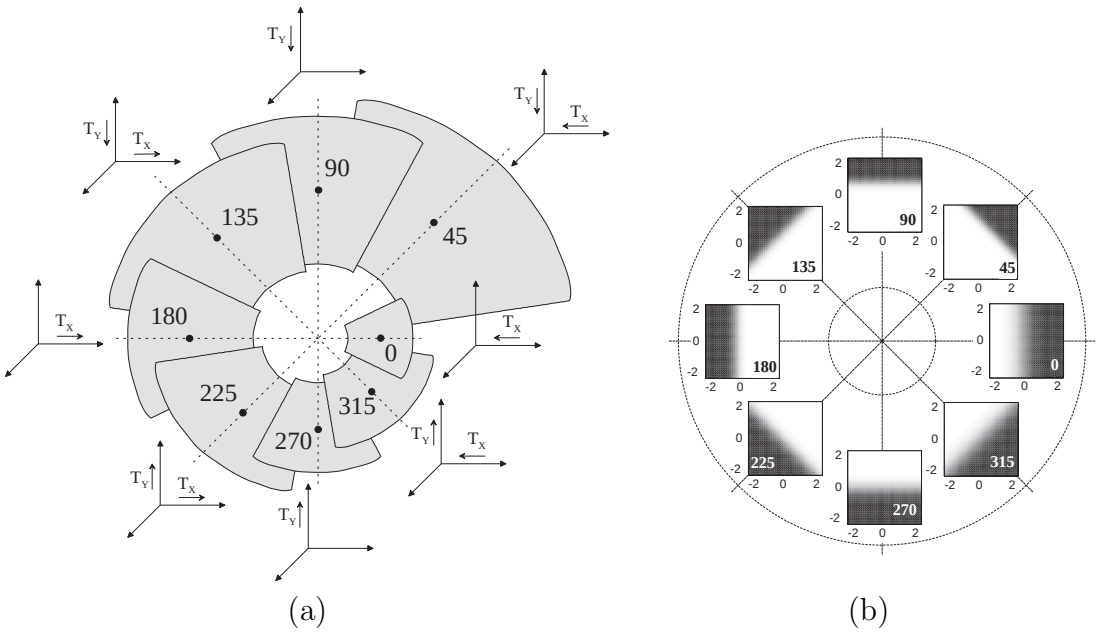

Figure 4: (a) The arrows on the reference frames show that for an expansion cell selectivity in terms of heading parameters changes with the position of the receptive field. (b) Single cell response contributions to the population encoding of the perceived heading (see text).

Accordingly, for each position on the cortical plane, cells are selective to a specific combination, of $\frac{T_X}{T_Z}$ and $\frac{T_Y}{T_Z}$. Fig. 4 shows the responses of a set of expansion cells, whose receptive field centers vary along a spiral on the retinal plane. Cells' responses increase steadly with the intensity of the velocity components; keeping fixed $(T_X^2 + T_Y^2)$ and T_Z, each cell has a maximal response for a preferred heading direction, as evidenced in the related coordinate frames shown in the figure. By construction, the preferred heading direction of each cell is always along the line joining its receptive field center to the gaze. By analyzing their responses as a function of $\frac{T_X}{T_Z}$ and $\frac{T_Y}{T_Z}$we can evidence how single cell responses in the model contribute to the population encoding of the perceived heading. The responses for expansion selective cells, whose receptive field centers are localized as in Fig. 4a, are shown as greyscale maps in Fig. 4b. Brightest regions indicate, through the pairs $(\frac{T_X}{T_Z}, \frac{T_Y}{T_Z})$ the positions of the centers of motion which elicit the highest cells' responses. According to their receptive field locations, cells are selective to centers of motion that are shifted in different positions in the visual field. By example an expansion selective cell with its receptive field at $\theta = 45^o$ maximally responds when the center of motion is located in the lower left hemifield.

The locus of headings compatible with a given response level of a cell is a line in the $(\frac{T_X}{T_Z}, \frac{T_Y}{T_Z})$ plane; this line represents a sort of heading constraint. Therefore, this implies that the response of a single model cell is not sufficient to fully estimate heading direction. The combination of the responses of different cells gives the intersection of these constraint thus disambiguating the true direction of heading. Similar results can be obtained in more realistic motion situations such as locomotion parallel to a ground plane and during fixation tasks.

4 Concluding remarks and perspectives

In this paper we propose a computational model for heading estimation in which the analysis of the optic flow is carried out directly in the space-time domain, by means of a spatiotemporal wave-like representation of the velocity field which allows us to avoid explicit vectorial operations in the parametric (i.e., velocity) space. In this way, vector calculus operations can be interpreted, with a good approximation, as spatiotemporal filtering operations which determine the direction of motion of the wave-like representation of the optic flow. The model is similar to other template models [Perrone and Stone, 1998] [Grossberg *et al.*, 1998], but it differs from them in two respects: our MST cells are speed tuned, and the templates are made of portions of elementary flow components (expansion, rotation) always centered on the fovea. Accordingly, for each model cell the best stimulus should be centered on the fixation point; even though different stimulus configurations can trigger a cell response, provided that the sub-pattern of the optic flow locally matches the cell preferences for motion component and speed. In a hierarchical perspective, our MST cells can be considered as basic units whose responses can be combined to obtain more powerful descriptors characterized by larger field aggregate selectivity. Basically, the role of lower-level MST neurons in interpreting optic flow fields would be one of responding to visual motion according to the degree of match between the visual input and the preferred optic flow field of the neuron, whereas a qualitative analysis of the fundamental features of optic flow (e.g., the detection of differential invariants) would be the role of higher-level MST neurons.

These considerations suggest that the numerous, and sometimes contradictory physiological cell properties relating MST cell response to the placement of optic flow stimuli in the visual field, including position invariance, center-of-motion tuning, direction reversals, could be re-examined from this new (gaze-centered) perspective. The center-symmetric selectivity preference of MST units could be also related to an "ecological" requirement in connection with their capability of judging heading direction and time-to-collision. A direct consequence of the gaze-centered representation is, indeed, the observation of maximal distribution of activity on MST layer when the preferred component is centered on the fixation point (see Fig. 3). This emphasis on central vision may have important implications for visual navigation since the direction of motion would most likely be foveated.

From an implementation point of view, these processing schemes can be made isomorphic to the behaviour of an analog architecture based on structured arrays reacting collectively to spatiotemporal input stimuli that can be directly implemented in VLSI, as demonstrated by recent prototypes of our group [Raffo *et al.*, 1998].

Acknowledgments

This work was partially supported by the *UNIGE-2000 Project "Spatio-temporal Operators for the Analysis of Motion in Depth from Binocular Images"*.

References

[Duffy and Wurtz, 1991] C. J. Duffy and R. H. Wurtz. Sensitivity of MST neurons to optic flow stimuli. I. A continuum of response selectivity to large-field stimuli. *J. Neurophysiol.*,

65:1329–1345, 1991.

[Dyre and Andersen, 1997] B.P. Dyre and G.J. Andersen. Image velocity magnitudes and perception of heading. *J. Exp. Psych.*, 23:546–565, 1997.

[Gibson, 1950] J.J. Gibson. *The perception of the visual world.* Riverside Press, Cambridge, 1950.

[Graziano *et al.*, 1994] M.S.A. Graziano, R.A. Andersen, and R.J. Snowden. Tuning of MST neurons to spiral motion. *J. Neuroscience*, 14:54–67, 1994.

[Grossberg *et al.*, 1998] S. Grossberg, E. Mingolla, and C. Pack. A neural model of motion processing and visual navigation by cortical area MST. Technical Report CAS/CNS-TR-97-015, Dept. of Cognitive and Neural Systems, Boston, MA, 1998.

[Heeger and Jepson, 1990] D.J. Heeger and A. Jepson. Visual perception of three-dimensional motion. *Neural Comp.*, 2:129–137, 1990.

[Koenderink, 1986] J.J. Koenderink. Optic flow. *Vision Res.*, 26:161–180, 1986.

[Kohler, 1947] W. Kohler. *Gestalt Psychology.* Liverright Press, 1947.

[Orban, 1992] G.A. Orban. The analysis of motion signals and the nature of processing in the primate visual system. In *Artificial and Biological Vision System*, pages 24–56. ESPRIT BR Series, Springer, Cambridge, 1992.

[Perrone and Stone, 1998] J.A. Perrone and L.S. Stone. Emulating the visual receptive-field properties of MST neurons with a template model of heading estimation. *J. Neuroscience*, 18:5958–5975, 1998.

[Raffo *et al.*, 1998] L. Raffo, S.P. Sabatini, G.M. Bo, and G.M. Bisio. Analog VLSI circuits as physical structures for perception in early visual tasks. *IEEE Trans. Neural Net.*, 9(6):1483–1494, 1998.

[Schwartz, 1977] E.L. Schwartz. Spatial mapping in primate sensory projection: analytical structure and relevance to perception. *Biol. Cybern.*, 25:181–194, 1977.

[Tanaka and Saito, 1989] K. Tanaka and H. Saito. Analysis of motion of the visual field by direction, expansion/contraction, and rotation cells clustered in the dorsal part of the medial superior temporal area of the macaque monkey. *J. Neurophysiol.*, 62:626–641, 1989.

[Tistarelli and Sandini, 1993] M. Tistarelli and G. Sandini. On the advantages of polar and log-polar mapping for direct estimation of time-to-impact from optical flow. *IEEE Trans. Pattern Anal. Mach. Intell.*, 15:401–410, 1993.